Shock-wave induced compressive stress on alumina ceramics by laser peening

Shukla, P., Crookes, R. & Wu, H.

Original citation:
Shukla, P, Crookes, R & Wu, H 2019, 'Shock-wave induced compressive stress on alumina ceramics by laser peening' Materials & Design, vol. 167, no. 107626
https://dx.doi.org/10.1016/j.matdes.2019.107626

DOI 10.1016/j.matdes.2019.107626
ISSN 0261-3069
ESSN 0264-1275

Publisher: Elsevier

Materials and Design 167 (2019) 107626

Contents lists available at ScienceDirect

Materials and Design

journal homepage: www.elsevier.com/locate/matdes

Shock-wave induced compressive stress on alumina ceramics by laser peening

Pratik Shukla [a,*], Robert Crookes [b], Houzheng Wu [b]

[a] School of Mechanical, Aerospace and Automotive Engineering, Faculty of Engineering, Environment and Computing, Coventry University, Priory Street, Coventry CV1 5FB, United Kingdom
[b] Department of Materials, Loughborough University, Loughborough LE11 3TU, United Kingdom

HIGHLIGHTS

- Local plastic deformation in ceramics can be created *via* laser shock peening (LSP).
- LSP of Al_2O_3 Ceramics was applied at 19.9; 29.85 and 33.83 GW/cm^2.
- Net compressive stress ranged from 104 to 168 MPa using above laser intensities.
- Dislocation density averaged 2.1 × 10^{13} and peaked to 2.0 × 10^{14} 1/m^2 at 29.85 GW/cm^2.

GRAPHICAL ABSTRACT

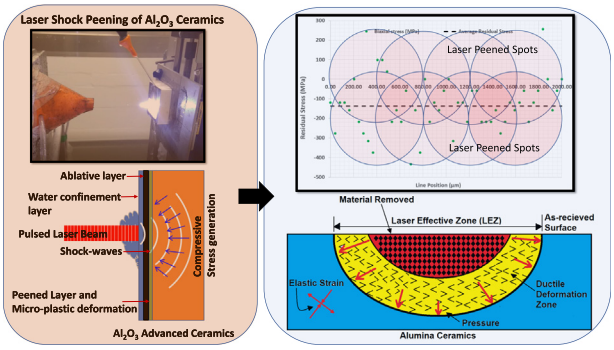

ARTICLE INFO

Article history:
Received 8 September 2018
Received in revised form 26 January 2019
Accepted 28 January 2019
Available online 30 January 2019

Keywords:
Laser shock peening: ceramics
Residual stress
Compression
Plasticity

ABSTRACT

Laser shock peening (LSP) of Al_2O_3 advanced ceramics is reported, showing underpinned physical mechanisms and potential benefits. It is known that localised plastic deformation can be induced in ceramics in the presence of a high hydrostatic pressure. It is therefore of high interest to apply LSP on large surface areas on ceramics in order to create a strengthening mechanism. An Nd: YAG laser was used for the study at an increment of 1 J, 1.5 J and 1.7 J laser energy. The LSP surface treatment was characterized using a 3-D surface profiler and a Cr^{3+} fluorescence spectroscopy from which residual stress and dislocation densities were determined after mapping with acquired Cr^{3+} fluorescence spectra. The results showed an increase in roughness by 10% at 1 J, to 62% at 1.5 J, and 95% at 1.7 J of laser energy. The net compressive stress increased from 104 MPa at 1 J, to 138 MPa at 1.5 J and 168 MPa at 1.7 J. The highest dislocation density was 2.0 × 10^{14} 1/m^2 and an average of 2.1 × 10^{13} 1/m^2 within the low compression zone at 1.5 J of laser energy. These results have shown a way forward to not only generate local plastic deformation, but open up a new avenue towards strengthening ceramics using laser peening technology.

1. Introduction

Alumina (Al_2O_3) is a widely used ceramic with its applications spanning in all types of industrial sectors. This is because of the superior mechanical and electrical properties that the material offers. However, crack sensitivity and brittleness prevent ceramics to depict the same benefits that metals offer, and therefore, strengthening ceramics in general has always been desirable and a necessity which directly impacts many applications in medical, automotive, military and nuclear industries. Laser shock peening introduces laser plasma-driven shock-waves into a material and such shock-waves create high pressure pulse [1]. These shock-waves consequently have the tendency to generate plastic deformation and induce compressive residual stress as a potential

* Corresponding author.
E-mail address: pratik.shukla@coventry.ac.uk (P. Shukla).

https://doi.org/10.1016/j.matdes.2019.107626

strengthening mechanism, particularly in metals and alloys [2–4]. To-date, the common knowledge is that ceramics cannot be plastically deformed, particularly with the use of laser shock peening. The mechanistic understanding of the topic is still one of the unreported and unknown topics. With that said, strengthening ceramics with laser shock peening is extremely beneficial because for instance, it's applicability could expand to enhancing the wear resistance of dental ZrO_2. Since their properties are poor under tensile loading, laser shock peening will also enable improved performance of these ceramics for dental applications. In addition, beneficial design changes can also be included to the design of armour ceramics, whereby, thinner bullet proof vests can render equal amount of strength as that of a thicker and a heavier product. Laser shock peening induced compressive stress will enhance the strength and in doing so will result to lighter ceramic armours that will equally perform well compared to a conventional one, but will reduce the physical struggle and fatigue for the end-user.

Only handful of papers can be found in the area of peening ceramics [4–13]. Koichi et al. [6], Schnick [7], Wang et al. [8–10], and the preliminary work of Shukla et al. on Si_3N_4, Al_2O_3 and SiC advanced ceramics [11–15], are the limited publications that are reported in the area of laser peeing ceramics. The work of Koichi et al. employed a Nd: YAG laser at a wavelength of 532 nm for the peening experiments and reported that an increase in surface roughness as the laser intensity was increased. As result, plastic straining was induced into the Si_3N_4 with compressive residual stress. Schnick et al. [7], conducted a study on Al/SiC composite coatings and mentioned that the coatings comprised of less porosity with improvement in the wear characteristics after laser shock peening was conducted. Compressive residual stresses were also reported to a depth of 1.2 mm in the work of Wang et al. [8] and in later publication, they reported dislocation and twin boundaries resulting to localised plastic deformation and grain boundary strengthening [9,10]. The work of Pfeiffer and Frey [16] and Pfeiffer and Wenzel [17], showed that significant level of compressive stress (around 900 MPa) can be induced into Si_3N_4 ceramics using the traditional shot peening technique. Furthermore, Ti-based bulk metallic glasses can be considered difficult to process due to its high stiffness and lower ductility than standard metals and alloys. Wang et al. [18] reported that laser shock peening in Ti-bulk metallic glass can induce sub-surface residual stress that is as much as −170 MPa and −350 MPa in X and Y direction. The depth of the compressive stress zone increases from 400 μm to 500 μm with increasing LSP treatment. The highest near-surface residual stress is about −750 MPa. Further, plastic deformation was also reported in bulk metallic glass substrate by other investigators [19,20]. With all said, investigations, particularly on laser shock peening of ceramics have not showed full range of parameters which could first produce crack-free regions over large surface area and render the possibilities to plastic deformation within the ceramics. This work on the other hand investigates, three different parameters to laser shock peen an Al_2O_3 over large surface area and particularly investigates the residual stress using a Cr^{3+} fluorescence method which is rather new for laser shock peening studies in general. In addition to this, a mechanistic understanding is also given which enable one to then deploy laser shock peening for strengthening advanced ceramics at a broader scale.

Plastic deformation in ceramics is a long going research topic. This is not only because it is challenging to bring about the effect of plastic deformation into ceramics, but also because having done so will open new avenue for these advanced materials. As such they can be applicable in areas where metallic systems fail due to lower mechanical properties than those offered by advanced ceramics [4,13–15]. The work of Longy and Cagnoux [21], first reported the generation of dislocation twins during a high velocity impact on Al_2O_3 armour ceramic. An increase in strength was found in the work of Wu et al. [22], after grinding and polishing Al_2O_3 matrix composites. Deformation of alumina at high strain-rate was reported in the work of Acharya et al. [23]. They indicated that these brittle materials can also undergo plasticity, dislocations and induction of compression [23]. In an attempt to study the compressive failure mechanism at low strain-rates, Bhattacharya et al. [24], reported 40% enhancement in compressive stress with increase in strain level which inherently, multiplied the dislocation presence, resulting in microplasticity within a coarse-grain alumina ceramic. Wu et al. measured the residual stress distribution around indentation and scratches in a polycrystalline Al_2O_3 and Al_2O_3/SiC nanocomposite using the Cr^{3+} fluorescence microscopy technique. The technique used was reported to be in good agreement and consistent with other experimental methods. It also showed that both plastic deformation and prediction of dislocation density can be tabulated using the broadening of the peaks of the Cr^{3+} fluorescence spectra [25]. Severe plastic deformation was also reported in a non-metallic substrate such as bulk metallic glass [26–28].

2. Experimentation

2.1. Laser shock peening

Laser shock peening was set-up (see Fig. 1), using a Q-switch 2.7 J, Nd: YAG laser (LPY7864-30, Litron Laser Ltd., Rugby, England). Fundamental wavelength of 1064 nm was used with a top-hat beam comprising of 0.5 mrad of divergence with an M^2 value of 1.99. The pulse energy was varied from 1 J, 1.5 J to 1.7 J leading on from our initial investigation that was performed at energy level under 1 J [15]. The spot diameter was kept constant at 0.8 mm and yielded a laser intensity from 19.9 to 33.83 GW/cm^2, respectively with a shock pulse pressure shown in Table 1. A pulse duration of 10 ns and a pulse repetition rate of 10 Hz was applied. Traverse speed was kept constant at 4.8 mm/s. The radiance density (the brightness of the laser) was determined based on the parameters shown in Table 1(b), using our previous method [26] and equated to 4.42, 6.63 and 7.52 (W/Cm^2/Sr/μm) respectively. A 50 mm by 50 mm laser peened patch was programmed for the three respective energies applied with a 50% overlap on the Al_2O_3 armour grade ceramics. The path of the laser beam was created in a zig-zag pattern as shown in Fig. 1. The sample was coated with a permanent black-ink coating which acted as an ablative and an absorptive layer. This was in-place of the conventional black tape that is normally used. A stream of water (see Fig. 1(a)) was made to flow over the sample material and was ranging at a thickness of 1 mm to 2 mm thickness.

2.2. Material details

Fine-grain armour grade Al_2O_3 ceramic (99%) plates manufactured as an armour plate, was used with a thickness of 9 mm, and a dimension of 100 mm × 100 mm. The Al_2O_3 armour ceramic tiles were as-sintered and consisted of 0.56 μm (Ra) original surface roughness on average. The Hugoniot Elastic Limit (HEL) was determined to be 7.98 GPa using the Eq. (4). Laser shock peening parameters can then be designed using the HEL and the required shock pulse pressure determined from the work of Peyre and Fabbro et al. [27]. The yield strength used was 560 MPa, Poisson's ratio of 0.23 [28], which ultimately equated to the HEL value, as found above for the Al_2O_3 ceramic. This meant that the shock pulse pressure to create the laser-plasma driven shock waves has to exceed the HEL of Al_2O_3 ceramic for plastic deformation to take effect based on the fact that the yield model developed for metal plasticity holds true for ceramics.

2.3. Residual stress measurement using Cr^{3+} fluorescence spectroscopy

Cr^{3+} fluorescence spectroscopy line scans were performed using a true confocal Raman microscope (Horiba, Japan) over a spectrum of 14,250–14,550 cm^{-1} with a 633 nm red line He-Ne laser. Changes to the local stress on a scale smaller than the sampling volume of the optical probe results to the broadening of the Cr^{3+} fluorescence line along the shift in the line, related to the mean hydrostatic stress of the sample

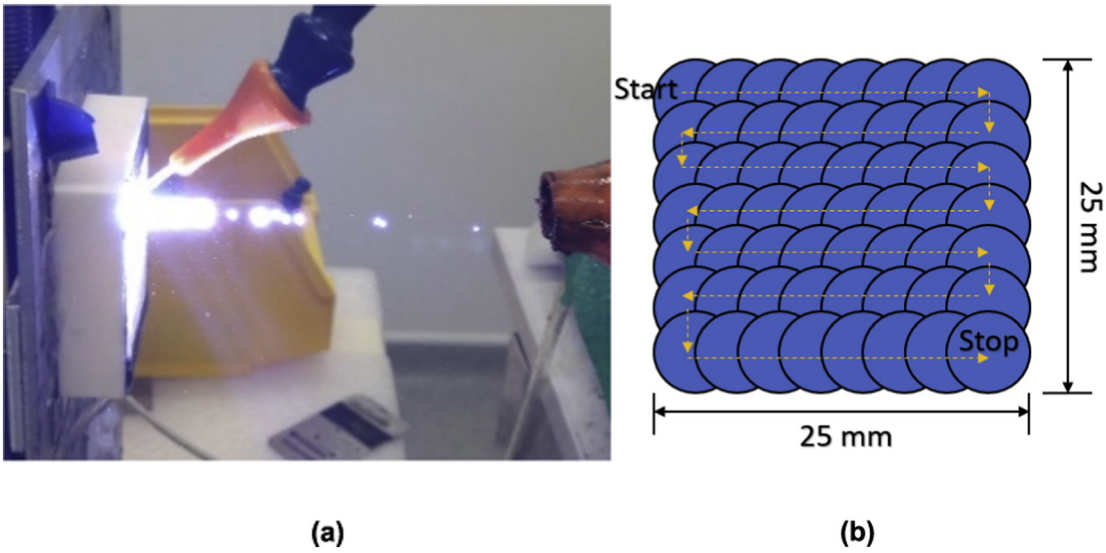

Fig. 1. illustrates with an optical image of the laser shock peening set-up in (a), and (b) laser beam path with peening strategy for the Al_2O_3 ceramic.

volume. This can be used to first determine the residual stress and also the dislocation density within the Al_2O_3 ceramic [25]. A ×50 objective lens was used, giving a spot size of 1 μm. Each of the spectra was collected twice for 1 s for a total detection time of 2 s. Line-scans were performed normal to the laser shock peening direction across 2 mm with a step size of 40.8 μm. A confocal setup allowed autofocus, ensuring that the spot remained focused over long line scans (see Fig. 2).

3. Results and discussion

3.1. Topography

As presented in Table 2 and Fig. 3(a), the average value of surface roughness Ra, prior to laser shock peening Al_2O_3 ceramic was 0.989 μm (untreated), whilst the laser shock peened surfaces increased in roughness to 1.08 μm at 1 J (Fig. 3(b)), 1.64 μm at 1.5 J (Fig. 3(c)), and 1.92 μm at 1.7 J (Fig. 3(d)). Surface roughening *via* laser shock peening usually results in material removal and is a by-product of the process. Based on the results herein, it can be gathered that the effects which occur with laser shock peening of metals (low carbon steel in particular [29], also occur with laser shock peening of Al_2O_3 ceramics with increased shock pressure. This is, whereby, the increase in the laser energy increases the thermal shock and thus, increases the material removal rate to 10%, 62%, and 95% as the laser energy increase. The melting of Al_2O_3 ceramic with laser shock peening is far from taking place as only 2041 °C [30] of heat is generated after being exposed to the laser energy for about 2.3 s (absorption of 1.06 μm wavelength with 12% absorption) at the highest applied energy 1.7 J) [31]. In this case, pulse duration was 10 ns, thus, the interaction temperatures would be much below that required to melt the Al_2O_3-causing unlikely phase changes to the Al_2O_3. This will eliminate the chance for material removal occurring from heating and melting process. Thus, it was predicted that the pressure pulse created the material removal and roughened topography. Maximum peak profile or height of the surface (Rp) was 6.59 μm for the as-received surface, but with increasing laser energies and in turn, the shock pressure, lead to a reduction in the surface roughness to 5.71 μm at 1 J, 6.07 μm at 1.5 J and 5.19 μm at 1.7 J. When comparing the as-received surface with the laser shock peened surface showed a reduced peak height of the surface, but the increase in this parameter from 1 J to 1.5 J, then a dipped when 1.7 J were applied. So further measurements are suggested to verify this finding. Although, the up and down change is likely due to statistical reasons, so choosing different sampling areas would be ideal. The root mean square roughness Rq was the lowest for the as-received surface, and as the energies increased, the Rq values began to increase as shown in Table 2. Maximum/total height of the profile (Rt) started with 27.24 μm and then increased with increasing energy. The values with respect to each level of laser energy were gradual and tied well with the fact that the surface roughening with increasing laser energy and respective pulse pressure created deeper craters on the surface. Likewise, to the positive surface roughness value, the negative surface roughness value of maximum profile valley depth (Rv) were in a reasonable agreement with the rest of the topographical effects in Table 2, whereby, the depth of roughness profile increased as the material removal increased with higher energies in comparison to the untreated surface.

Table 1
showing the experimental parameters for laser shock peening of Al_2O_3 ceramic.

Parameters	Values
Pulse energy (J)	1 J, 1.5 J, 1.7 J
Laser power intensity (Gw/cm^2)	19.9 @ 1 J
	29.85 @ 1.5 J
	33.83 @ 1.7 J
Shock pulse pressure (GPa)	7.58 @ 1 J
	9.29 @ 1.5 J
	9.89 @ 1.7 J
Radiance density (W/Cm^2/Sr/μm)	4.42 @ 1 J
	6.63 @1.5 J
	7.52 @ 1.7 J
Spot diameter (mm)	0.8
Pulse repetition rate (Hz)	10
Over lapping rate (%)	50
Pulse duration (ns)	10
Wavelength (nm)	1064
Traverse speed (mm/s)	4.8
Hugoniot elastic limit (GPa)	7.98

3.2. Global residual stress on the laser shock peened surfaces

The maximum compressive stress measured on the surface after laser shock peening with 1 J was – 276 MPa and the maximum tensile stress was 39.53 MPa, which rendered an average stress of −100 MPa over a length of 2 mm as presented in Fig. 4(a). On the surface treated with 1.5 J, the maximum compressive stress measured was −434 MPa and a maximum tensile of 98.81 MPa; an average residual stress of −138 MPa was measured over a length of 2 mm, as illustrated in Fig. 4(b). The Al_2O_3 laser shock peened surface with 1.7 J yielded a maximum compressive stress of −494 MPa which was the highest from the

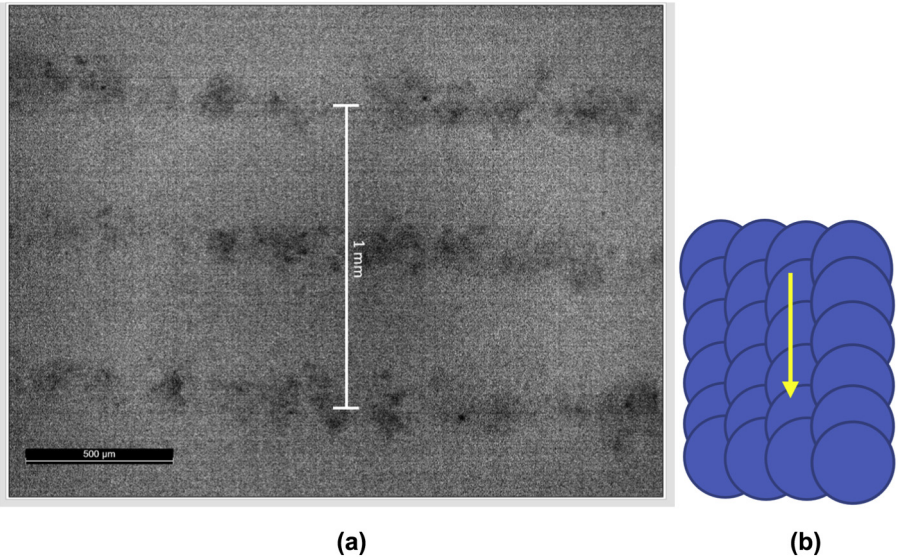

Fig. 2. (a) An optical image from the confocal microscope showing the peened area and scanned region; (b) schematic of the path of the fluoresence line-scan over the laser peened areas.

three energies applied. The maximum tensile stress on this surface was 158 MPa with an average stress of −168 MPa as illustrated in Fig. 4(c). From the three peened surfaces, it was observed that, with the laser energy increased, an increase in the average compressive stress also resulted. An obvious explanation for that was due to the increase in laser plasma-driven shock waves from the increased shock pulse pressure *via* the increase in laser energy and in turn, the laser power intensity that boosted the level of compressive stress. The use of Cr^{3+} fluorescence technique to measure residual stress was also previously adopted by Wu et al. [32]. They stated that the distribution of stress around indentation probe (cold, mechanical impact) ranged from 450 MPa to 550 MPa in compression within an Al_2O_3 ceramic, which is equivalent to the levels measured on the surfaces of laser shock peened Al_2O_3. However, Wade et al. had used contact impact with slightly higher energy input than the ones in this work (2.98 J) and was over an approximate contact diameter of 200 µm [32]. This was applied with higher energy density than the one in this study, thus, it led to higher induced damage such as extensive cracking, apart from similar level of residual compressive stress.

3.3. Residual stress pattern on laser shock peened surface

A representative biaxial residual stress map for the laser peened surface at 1.7 J is shown in Fig. 5, where the laser peening track is indicated by a dashed line. Inside the laser peened spot within the patch, the residual stress is dominated by a low-level compression, at a level around −350 MPa (see arrow in Fig. 5(a)), hence, called low compression zone (LCZ). Low level tensile stress is also detected at some positions inside LCZ. Based on the spreading of low-level compression along the Y-axis, we estimate the lower and upper bound of this LCZ track are around 200 and 700 µm, respectively. Such an uneven width of LCZ laser shock peened track should be associated with the peened effective zone (PEZ) size of each laser spot and the overlap between adjacent laser spots, which will be discussed further.

In the region surrounding the LCZ track, as indicated by two dark dashed lines, the residual stresses at all detected positions are dominated by compression, but at a significantly higher level than those inside the LCZ peened track. At most of the positions, the compression was around 300 to 500 MPa. Some positions gave compression levels up to ~550 MPa, and some as low as 40 MPa under tension. We call this region a high compression zone (HCZ). Due to the limitation of mapping view, we cannot show the full width of the HCZ, but a width of more than ~500 µm is shown in Fig. 5(b).

The experimental measurements of the shift of Cr^{3+} fluorescence peak have provided a clear evidence proving that a laser shock peened surface of the Al_2O_3 ceramic was under compression overall. Without chemical modification of alumina crystal lattice, such compression may come from (a) ductile deformation, and/or (b) quenching effect. However, with the laser peening pulse duration being 10 ns, the temperatures are much lower (exhibiting a cold surface treatment), thus, the laser peened Al_2O_3 would not be subject to quenching and so quenching would have no contribution to the residual surface compression. On one hand, heating up of Al_2O_3 ceramic *via* the laser, if any at all is on the surface and the rest of the ceramic is cold, hence, quenching itself does not produce tempering effect as widely adapted to toughening glass. In addition, quench doesn't lead to any phase transformation as seen with high carbon steel [33], or zirconia toughened ceramics [30]. Hence, only ductile deformation may result from may the surface compressive origin induced from the pressure generated *via* the shock wave.

To examine if ductile deformation occurred on the surface of the Al_2O_3 ceramic; we measured the broadening of Cr^{3+} fluorescence spectroscopy. Wu et al. have established a quantitative correlation between dislocation density, ρ, in alumina crystal and net broadening, δμ, of Cr^{3+} fluorescence peak when other factors are excluded for possible broadening contribution, as shown in Eq. (1) below:

$$\sqrt{(\delta\mu^2)} = K\sqrt{f\ F\ (\rho)} \tag{1}$$

where K is a factor determined by the elastic modulus and piezo-spectroscopic coefficient of alumina, *f* is the fraction of the illuminated

Table 2
Presents 2-D surface roughness characteristics of the Al_2O_3 ceramic prior-to and post laser shock peening.

Surface condition	Surface roughness (Ra)				
	Ra (µm)	Rp (µm)	Rq (µm)	Rt (µm)	Rv (µm)
As-received	0.989	6.59	1.33	27.24	−20.64
1 J	1.082	5.71	1.65	28.46	−22.74
1.5 J	1.64	6.079	2.73	29.45	−23.37
1.7 J	1.92	5.19	3.10	30.54	−25.35

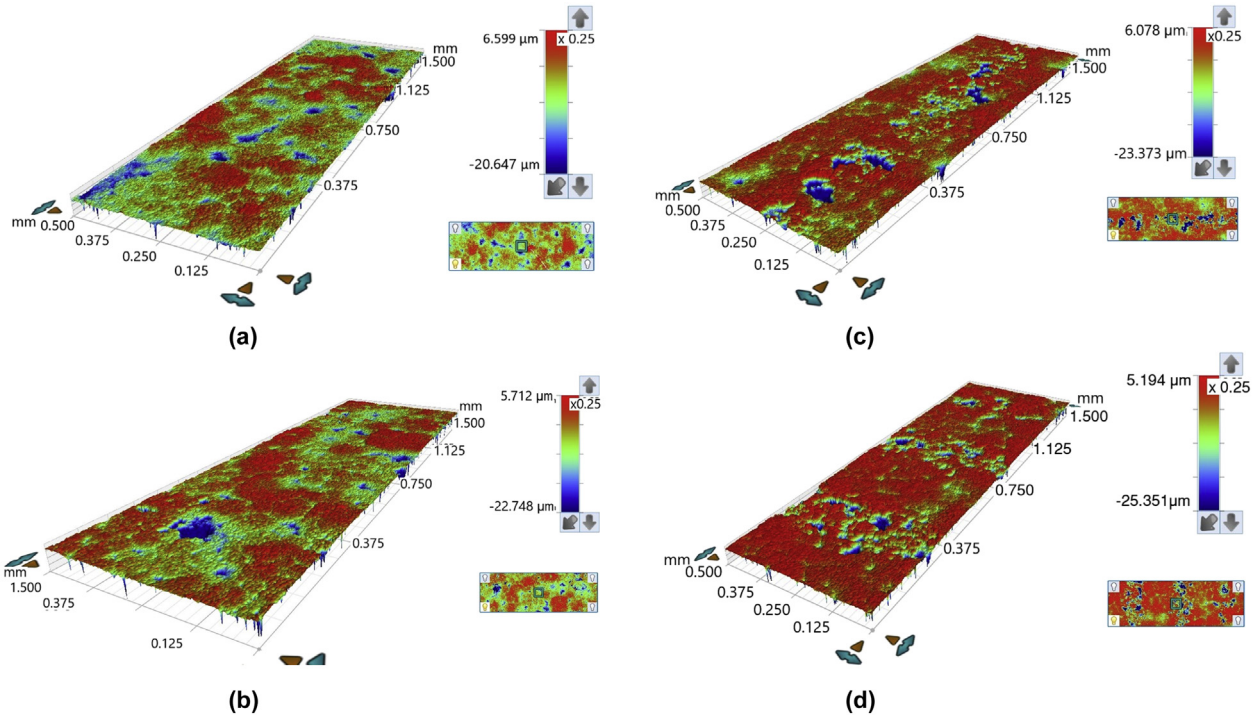

Fig. 3. Showing an illustration of a 3-D profile of the untreated Al_2O_3 ceramic in (a); the laser shock peened surface with 1 J in (b); laser shock peened surface with 1.5 J in (c) and the laser shock peened surface with 1.7 J in (d).

volume that contains the surface region of constant dislocation density, and F(ρ) is a function of dislocation density expressed as Eq. (2):

$$F(\rho) = \sqrt{\rho \, In \, (1/b\sqrt{\pi\rho})} \tag{2}$$

where b is the Burger' vector of dislocation.

The measured broadening map is shown in Fig. 5(b). There are 3 discrete regions showing significant broadening with δFWHM up to 5 cm^{-1}. Beyond these three regions inside this mapped area, the net broadening is zero. These regions giving broadening of the Cr^{3+} fluorescence peaks are approximately circulated by white dashed lines, labelled as A, B and C. In this map, region B shows the broadening inside a full spot impacted by one laser pulse, and A and C give only part of the represented full spots.

By carefully looking at region B, it is clear that the broadening of the Cr^{3+} fluorescence peak is highly inhomogeneous inside a spot, ranging from <1 up to 5 cm^{-1}. It appears that large broadening happened in the central area which is surrounded by a lower broadening region. With the measurements of net broadening, we have estimated using Eq. (1) that the highest dislocation density developed by laser shock peening was 2.57×10^{13} $1/m^2$. Such dislocation density is close to the highest measured inside a residual impression after indented by a sharp Vickers indenter [25]. The lowest density was about 8.37×10^{10} $1/m^2$. This is a similar scenario measured inside an indentation impression [25].

The variation of measured dislocation density is likely due to the inhomogeneous ductile deformation inside a polycrystalline alumina, as supported by the following reasons. For a polycrystalline material, a minimum of 5 independent active slip systems are required to accommodate geometric deformation in the 3-dimentional space when it is under non-isostatic hydraulic loading conditions [35–37]. For alumina crystal, the easily activated slip systems are those along basal plan, *i.e.* 1/3<1-210> (0001), at a low temperature region. To activate slips along rhombohedral and prism planes, a much higher critical shear stress is required, if microcracking can be restrained. Hence, under normal loading conditions, there are not enough independent slip systems in alumina to fully accommodate mechanical deformation at lower temperature regime [38,39]. That said, when the temperature is high enough, for instance >1100 °C as experimentally demonstrated by Heuer et al. [40], non-basal dislocations can be activated and glide under much lower shear stress. In this study, we assume the temperature is low enough due to water cooling and the laser pulse duration being in the ns pulse regime; the only slips along basal planes can be activated and glided. Hence, under the compression conditions generated by the shock pulses, only those grains, whose basal planes are aligned to the shear stresses, that are subject to shear stress higher than the critical shear stress, can be deformed through the glide of dislocations. Other grains may have no dislocation activated due to a fact that shear stress is not high enough, or microcracking could happen along any weak positions such as grain boundaries, or internal pores.

The plasma pressure was first identified and was calculated using Eq. (3) [27]:

$$P_{max}(GPa) = 0.01\sqrt{\frac{\alpha}{2\alpha+3}}\sqrt{Z}\sqrt{I_0} \tag{3}$$

where P_{max} is the maximum peak pressure induced by plasma (GPa); α is the ratio of thermal to internal energy; Z is the reduced shock impedance between the Al_2O_3 and confinement medium (water) in our case. I_0 is the constant absorbed laser power density in the confined ablation mode [23].

Therefore, the plastic deformation due to the shock-wave produced by the LSP can be determined by Eq. (4) [1,27]:

$$HEL \, \frac{1-\nu}{1-2\nu} \, \sigma_y^d \tag{4}$$

where υ is the Poisson's ratio of the material, σ_y^d is the dynamic yield strength at high strain rates. Conventionally with metallic materials, the shock-wave spreads into the material and plastic deformation occurs up to a depth at which the peak stress induced on the material would equal to its HEL. The HEL is related to the dynamic yield strength at high strain rates, σ_y^d [1,27]. Eqs. (3) and (4) were used in order to calculate the plasma pressure, and the HEL of the Al_2O_3 ceramic (see

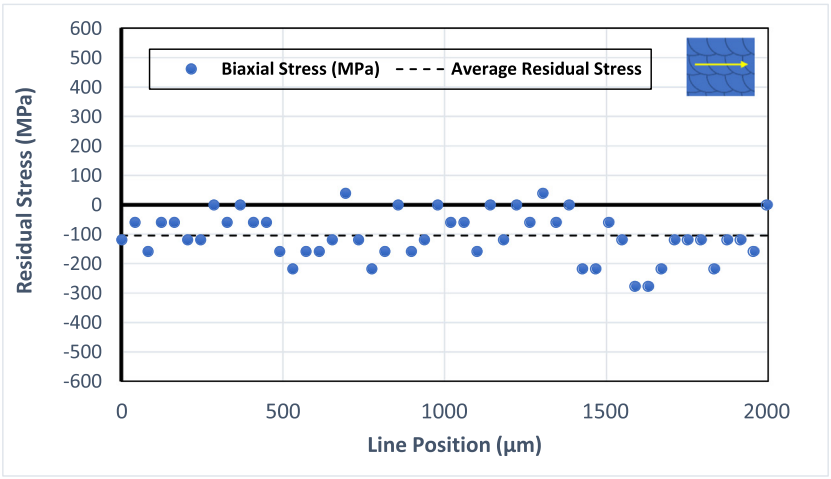

(a)

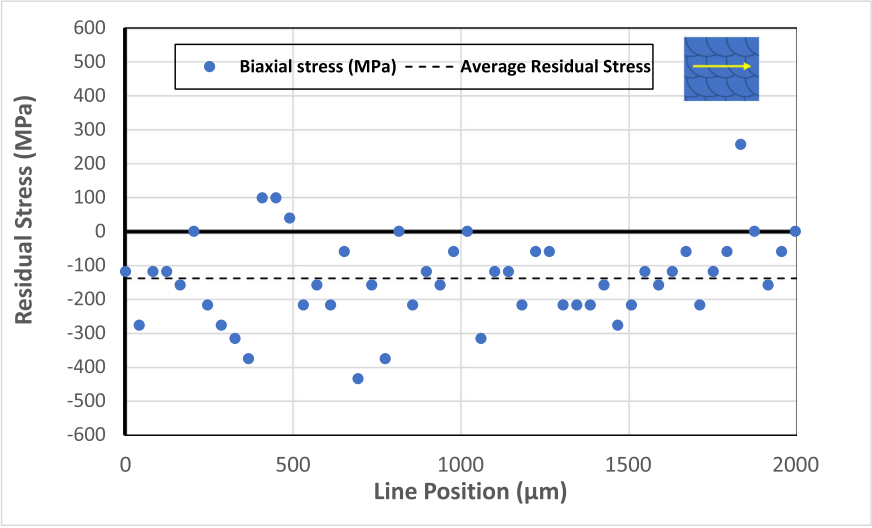

(b)

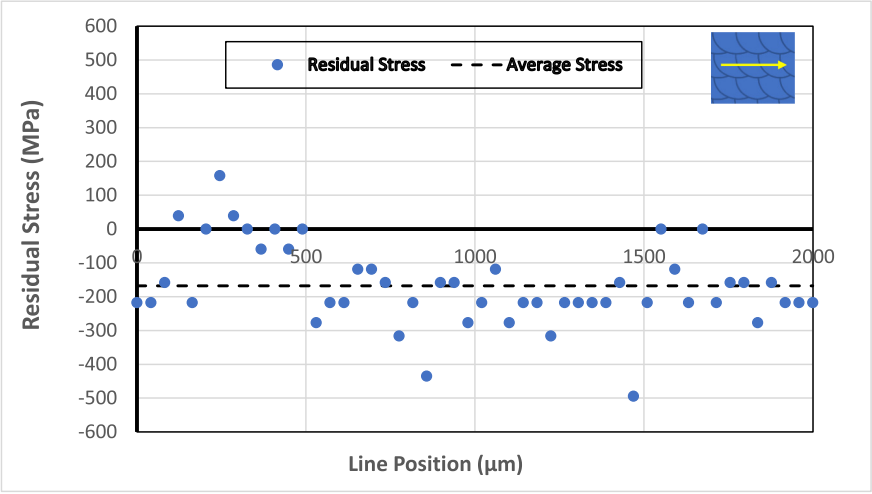

(c)

Fig. 4. Illustrating the residual stress after laser shock peening Al_2O_3 ceramics at 1 J in (a); at 1.5 J in (b); and 1.7 J in (c).

Table 1). Common knowledge for metallic materials suggests that for sufficient plastic deformation to take place, the HEL of the material should be exceeded by the pressure pulse to a required magnitude [1,27]. The HEL for the Al_2O_3 armour ceramic used for this study was somewhat equal or lower than the actual pressures applied by the laser parameters which was also indicative by the increase in dislocation activity based on the fact that yield model developed for metal plasticity also applied for ceramics which appears to be true from this work.

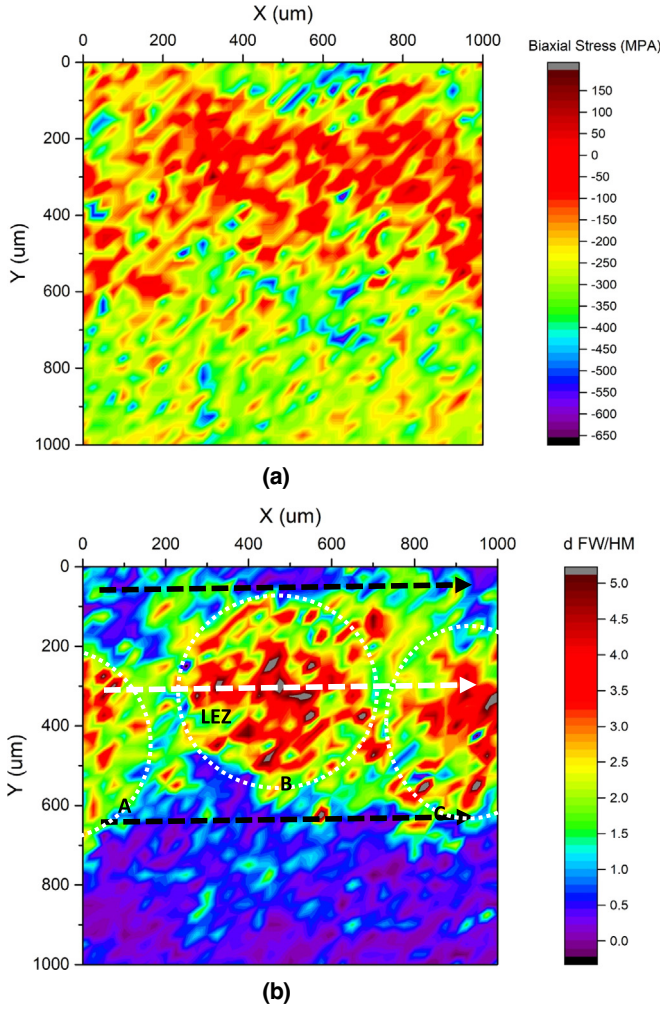

Fig. 5. Illustrates the Cr^{3+} fluorescence map of the residual stress over the surface in (a); through the cross-section in (b) for the Al_2O_3 ceramic laser shock peened at 1.7 J.

Furthermore, the general trend that the central region renders the highest dislocation density implicates that highest shear stress must be generated by the shock-waves inside this region. Following the transmission nature of a spherical shock-waves, the shear stress fades fast when a position is further away from the centre. We believe that fading of shear stress could be the key reason why a lower dislocation density region appears around the high dislocation core, and beyond this low dislocation region, the critical shear stress is not high enough to activate any dislocation, leading to no ductile deformation. The underpinned mechanisms for the observed ductile deformation, as well as the landscape of ductile deformation inside and around a peening spot are schematically shown in Fig. 6.

In order to know the depth profile of ductile deformation, a cross-section along the track was mapped with the variation of net broadening of a Cr^{3+} fluorescence peak. The results are shown in Fig. 6(a). Inside the view of this cross-section, two laser shock peened spots were applied, as circulated by white dashed lines. The largest broadening level is the same as that detected on the surface. Both broadening profiles of the peened spots showed that ductile deformation took place inside the hemispherical regions underneath the peening position. The large broadening in the central region occurred down to a depth of nearly 200 μm, and on the surface extended to a range of about 500 μm. Beyond the high broadening regions, the measurements imply that no ductile deformation is introduced by the shock wave due to shear stress level becoming too low by the fading of compression induced by shock-waves.

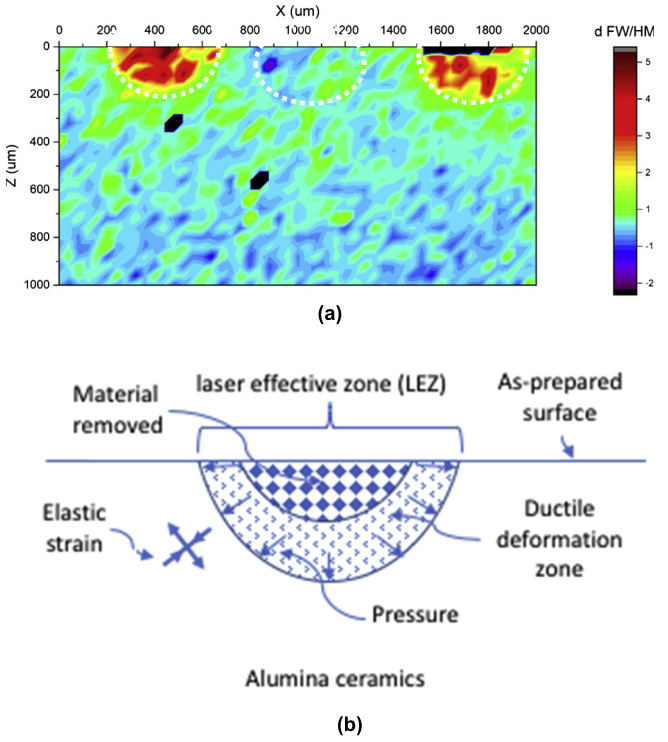

Fig. 6. (a) illustrates the full width half maximum (FWHM) peak over three overlapping spots in the cross-section in (b).

Based on the experimental measurements, we can establish the possible interaction that took place during laser shock peening of Al_2O_3 ceramics, as shown schematically in Fig. 6(b). The pressure waves generated by the laser shock peening deformed the Al_2O_3 with dislocations generated inside a region close to a hemispherical shape. Without boundary conditions accounted, the ductile deformation makes the laser effective region (LER) under hydraulic pressure, *P*, and the region around this LER is under elastic deformation. The material removal is obvious from the topographical images in Fig. 3 and Table 2, however, the depth of material removal in reality will not be as significant as shown in the schematic. With that said, it is yet a good representation of the effects that will take place during a nano second laser pulse with an Al_2O_3 ceramic surface under shock peening conditions.

4. Conclusions

The results presented in this paper revealed a new direction towards the use of laser shock peening to strengthen advanced ceramics such as Al_2O_3. This work shows cross-disciplinary research focused on the use of controlled laser pulses and its experimental set-up to strengthen difficult to process advanced ceramics. This technique is extremely beneficial as it impacts design changes that lead to cost reduction and simplicity, whilst maintaining the same level of strength for ceramics deployed for armour and dental applications for instance. The findings elucidated that upon increasing the laser energy, the surface roughness was increased to 10%, 62%, and 95% at 1 J, 1.5 J and 1.7 J respectively when the 3-D topography was compared with the untreated surface. As the laser energy increased the shock pulse pressure, the compressive stress also increased to an average of −104 MPa at 1 J, −138 MPa at 1.5 J and −168 MPa at 1.7 J. This was backed and verified by the considerable increase in dislocation density after laser shock peening. The density of dislocation is in localised peaks/bands rather than distributed evenly over the surface. In addition to that, the Cr^{3+} fluorescence line-scan comprised of a 1 μm diameter beam which detected only the localised peaks. Having said that, the average dislocation density at 1 J was found to be 6.11×10^{11}, and at 1.5 J was 2.67×10^{14} and 2.10×10^{13}

for 1.7 J respectively. The Cr^{3+} fluorescence mapping has illustrated plastic deformation and surface residual stress, introduced by the laser shock peening. The results found herein are very positive on the basis that a moderate compressive stress (in terms of Al_2O_3 ceramics) has been introduced into the surface. In addition, to the best of the authors knowledge, this is the first-time a detailed experimental result that has evidenced Cr^{3+} fluorescence mapping of laser shock peened Al_2O_3 ceramics. A comprehensive study detailing the cross-sectional profiles of plastic deformation and residual stress, as well as any cracking damage *etc.* is currently underway to address the full understanding of the laser shock peening process to treat difficult to process material such as ceramics.

Credit author statement

Houzheng Wu has contributed towards writing of the paper. Robert Crookes collected the residual stress data. Pratik Shukla planned the research, wrote the paper and undertook laser peening experiments.

Declaration of interest

It is confirmed that there are no actual or potential conflict of interest including any financial, personal or other relationships with other people or organizations within three years of beginning the submitted work that could inappropriately influence, or be perceived to influence, their work.

References

[1] A.K. Gujba, M. Medraj, Laser peening process and its impact on materials properties in comparison with shot peening and ultrasonic impact peening, Materials 7 (2014) 7925–7974.

[2] C.E.J. Dancer, H.M. Curtis, S.M. Bennett, N. Petrinic, R.I. Todd, High strain rate indentation-induced deformation in alumina ceramics measured by Cr^{3+} fluorescence mapping, J. Eur. Ceram. Soc. 31 (2011) 2177–2187.

[3] L. Louro, M. Meyers, Effect of stress state and microstructural parameters on impact damage of alumina-based ceramics, J. Mater. Sci. 24 (1989) 2516–2532.

[4] P.P. Shukla, T.P. Swanson, C.J. Page, Laser shock peening and mechanical shot peening processes applicable for the surface treatment of technical grade ceramics: a review, Proc. Inst. Mech. Eng. B J. Eng. Manuf. 228 (5) (2014) 639–652.

[5] M.W. Chen, J.W. McCauley, D.P. Dandekar, N.K. Bourne, Dynamic plasticity and failure of high-purity alumina under shock loading, Nat. Mater. 5 (2006) 614–618.

[6] A. Koichi, Y. Sano, T. Kazuma, T. Hirotomo, I.O. Shin, Strengthening of Si_3N_4 Ceramics by Laser Peening, Residual Stresses VII, 524–525, ECRS7, 2006 141–146.

[7] T. Schnick, S. Tondu, P. Peyre, L. Pawlowski, S. Steinhäuser, B. Wielage, U. Hofmann, E. Bartnicki, Laser shock processing of Al-SiC composite coatings, J. Therm. Spray Technol. 8 (2) (1999) 296–300.

[8] F. Wang, C. Zhang, Y. Lu, M. Nastasi, B. Cui, Laser shock processing of polycrystalline alumina ceramics, J. Am. Ceram. Soc. (2016) 1–7.

[9] F. Wang, C. Zhang, X. Yan, L. Deng, Y. Lu, M. Nastasi, B. Cui, Microstructure-property relation in alumina ceramics during post-annealing process after laser shock processing, Am. Ceram. Soc. 101 (11) (2018) 4933–4941.

[10] F. Fang, X. Yan, Y. Zhang, Y. Chenfei, M. Nastasi, B. Cui, Fundamental mechanisms of laser shock processing of metals and ceramics, Proceedings of SPIE-Advanced Laser Processing and Manufacturing II, 108130Q, 2018.

[11] P. Shukla, J. Lawrence, Laser Shock Peening of Si_3N_4 Ceramics: Experimental Set-up and General Effects, Science and Technology Facilities council (STFC) Annual Reports/article, 2014/2015 P40.

[12] P. Shukla, J. Lawrence, Alteration of Fracture toughness (K_{Ic}) of Si_3N_4 Advanced Ceramics by Laser Shock Peening, Science and Technology Facilities council (STFC) Annual Reports/article, 2014/2015 P41.

[13] P. Shukla, G.C. Smith, D.G. Waugh, J. Lawrence, Development in laser peening of advanced ceramics, Proc. SPIE 9657 (2015) 77–85.

[14] P. Shukla, S. Nath, W. Wang, W.X. Shen, J. Lawrence, Surface property modifications of silicon carbide ceramic following laser shock peening, J. Eur. Ceram. Soc. 37 (9) (2017) 1728–1739.

[15] P. Shukla, S. Robertson, H. Wu, A. Telang, M. Kattoura, S. Nath, S.R. Mannava, K. Vasudevan, J. Lawrence, Surface engineering alumina armour ceramics with laser shock peening, Mater. Des. 134 (2017) 523–538.

[16] W. Pfeiffer, T. Frey, Advances in shot peening of silicon nitride ceramics, International Conference and Exhibition on Shot Peening, ICSP9, Paris 2005, pp. 326–331.

[17] W. Pfeiffer, J. Wenzel, Shot peening of brittle materials – status and outlook, Mater. Sci. Forum 638–642 (52) (2010) 799–804.

[18] L. Wang, Z. Lu Wang, Y. Nie, H. Fu Ren, Evolution of residual stress, free volume, and hardness in the laser shock peened Ti-based metallic glass, Mater. Des. 111 (5) (2016) 473–481.

[19] C. Ma, S. Suslov, C. Ye, Y. Dong, Improving plasticity of metallic glass by electropulsing-assisted surface severe plastic deformation, Mater. Des. 165 (2019), 107581. .

[20] L.L. Wang, L.L. Wang, Z. Nie, Y. Ren, Y. Xue, R. Zhu, H. Zhang, H. Fu, Evolution of residual stress, free volume, and hardness in the laser shock peened Ti-based metallic glass, Mater. Des. 111 (2016) 473–481.

[21] F. Longy, K. Cagnoux, Plasticity and microcracking in shock-loaded alumina, J. Am. Ceram. Soc. 76 (1989) 971–979.

[22] H.Z. Wu, C.W. Lawrence, S.G. Roberts, B. Derby, The strength of Al_2O_3/SiC nanocomposites after grinding and annealing, Acta Mater. 46 (11) (1998) 3739–3748.

[23] S. Acharya, S. Bysakh, V. Parameswaran, A.K. Mukhopadhyay, Deformation and failure of alumina under high strain rate compressive loading, Ceram. Int. 41 ((2015) 6793–6801.

[24] M. Bhattacharya, S. Dalui, N. Dey, S. Bysakh, J. Ghosh, A.K. Mukhopadhyay, Low strain rate compressive failure mechanism of coarse grain alumina, Ceram. Int. 42 (2016) 9875–9886.

[25] H. Wu, S.G. Roberts, B. Derby, Residual stress distributions around indentations and scratches in polycrystalline Al_2O_3 and Al_2O_3/SiC nanocomposites measured using fluorescence probes, Acta Mater. 56 (2008) 140–149.

[26] P. Shukla, J. Lawrence, Y. Zhang, Understanding laser-beam brightness: a review on a new prospective in materials processing, Opt. Lasers Eng. 75 (2015) 40–51.

[27] P. Peyre, R. Fabbro, Laser shock processing: a review of the physics and applications, Opt. Quant. Electron. 27 (1995) 1213–1229.

[28] Granta Design Ltd. CES 2017 Selector, Edu-Pack, Cambridge, UK, 2017www.granta.co.uk.

[29] J.P. Chu, J.M. Rigsbee, G. Banas, H.E. Elsayed-Ali, Laser-shock processing effects on surface microstructure and mechanical properties of low carbon steel, Mater. Sci. Eng. A 260 (1999) 260–268.

[30] R.C. Bradt, M. Ashizuka, T.E. Easler, H. Ohira, Statistical aspects of the thermal shock damage and the quench-strengthening of ceramics, in: G.A. Schneider, G. Petzow (Eds.), Thermal Shock and Thermal Fatigue Behavior of Advanced Ceramics. NATO ASI Series (Series E: Applied Sciences), 241, Springer, Dordrecht, 1993.

[31] Z. Zhang, M.F. Modest, Temperature-dependent absorptances of ceramics for Nd:YAG and CO_2 laser processing applications, Heat Transf. 120 (2) (1998) 322–327.

[32] J. Wade, S. Robertson, Y. Zhu, H. Wu, Plastic deformation of polycrystalline alumina introduced by scaled-down drop-weight impacts, Mater. Lett. (2016) 134–147.

[33] G.M. Martínez-Cázares, D.E. Lozano, M.P. Guerrero-Mata, R. Colás, G.E. Totten, High-speed quenching of high carbon steel, Mater. Perform. Charact. 3 (4) (2014) 256–267.

[35] H. Wu, S.G. Roberts, B. Derby, Residual stress and subsurface damage in machined alumina and alumina/silicon carbide nanocomposite ceramics, Acta Mater. 49 (2001) 507–517.

[36] H.Z. Wu, S.G. Roberts, G. Mobus, B.J. Inkson, Subsurface damage analysis by TEM and 3D FIB crack mapping in alumina and alumina/5vol.%SiC nanocomposites, Acta Mater. 51 (2003) (2003) 149–163.

[37] H. Wu, Understanding residual stresses and fracture toughness in ceramic nanocomposites, in: Mahmood M. Shokrieh (Ed.), Residual Stresses in Composite Materials, Woodhead Publishing, Cambridge 2014, pp. 256–292 , Chapter 10.

[38] S.P. Timoshenko, J.N. Goodier, Theory of Elasticity, 3rd ed. International student ed. New York, McGraw-Hill, 1970 (Textbook 567pages).

[39] M. Qing, R. David, S. Clarke, Piezospectroscopic determination of residual stresses in polycrystalline alumina, J. Am. Ceram. Soc. 77 (2) (1994) 585–597.

[40] A.H. Heuer, K.P.D. Lagerlöf, J. Castaing, Slip and twinning dislocations in sapphire (α-Al_2O_3), Philos. Mag. A 78 (3) (1998) 747–763.